Electronic Supplementary Material (ESI) for RSC Advances.

SUPORTING INFORMATION

CHARACTERIZATION OF PEPTIDE SELF-ASSEMBLY BY LOW FREQUENCY RAMAN SPECTROSCOPY

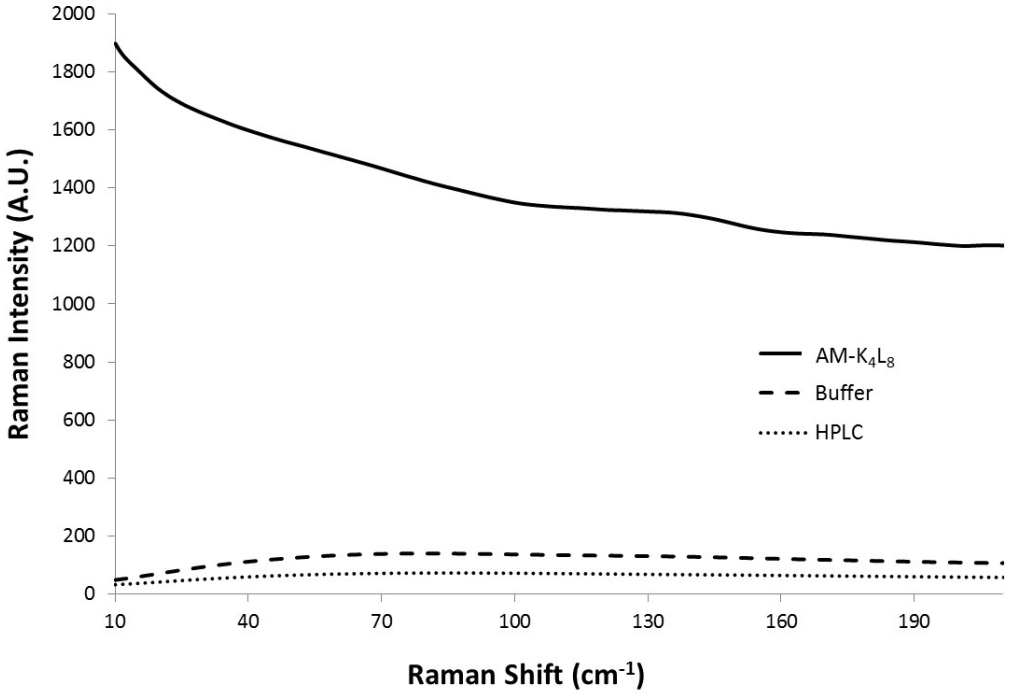

Figure S1: The raw LF-Raman intensity modes of HPLC-grade water and the dilution buffer (50% acetonitrile and 0.05 M HCl in HPLC-grade water) in comparison to AM-K_4L_8 model peptide.

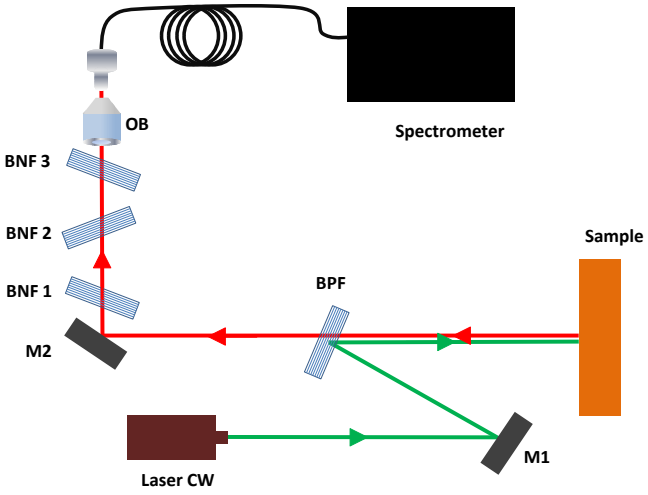

Figure S2: Schematic of Raman apparatus setup with band notch filters (BNF1-3) to reject the Rayleigh scattering by 9 orders of magnitude, clean-up bandpass filter (BPF) to clean the continuous wave (CW) laser beam, mirrors (M1-M2), and microscope objective (OB).

	Measurement 1		Measurement 2		Measurement 3		Measurement 4	
AM-K_4L_8 fiber	**Particle size (nm)**	**Intensity (%)**	**Particle size (nm)**	**Intensity (%)**	**Particle size (nm)**	**Intensity (%)**	**Particle size (nm)**	**Intensity (%)**
	248 (±26%) 1573 (±22%)	10% 90%	156 (±33%) 846 (±27%) 2667 (±35%)	14% 25% 61%	 515 (±4.5%) 2385 (±4%)	 42% 58%	136 (±20%) 370 (±9.4%) 3616 (±7%)	7% 44% 49%
AM-[D]-L4,10 crystal	**Particle size (nm)**	**Intensity (%)**	**Particle size (nm)**	**Intensity (%)**	**Particle size (nm)**	**Intensity (%)**		
	1086 (±9.1%) 10000 (1%)	45% 55%	951 (±4.5%) 8960 (±3%) 10000 (3%)	82% 5% 13%	503 (±10%) 7404 (±17%)	47% 53%		
AM-[D]-K2,11 intermediate morphology	**Particle size (nm)**	**Intensity (%)**	**Particle size (nm)**	**Intensity (%)**	**Particle size (nm)**	**Intensity (%)**		
	118 (±14%) 518 (±8%) 5234 (±12%)	4% 48% 48%	112 (12%) 624 (±21%) 7940 (27%)	5% 70% 25%	 475 (±5%) 4206 (±5%)	 47% 53%		

Table S1: Mean particle size, particle size distribution and intensity of amphipathic set of diastereomeric peptides measured with DLS apparatus. The examples emphasize the large variability between the measurements due to inherent stochasticity of self-assembling aggregation. In our case, the DLS analysis is more qualitative than quantitative, describing the aggregation tendency of amphipathic model peptide and its structural diastereomers. The measurements were performed in triplicates using 2.5 mg/ml of each sample.

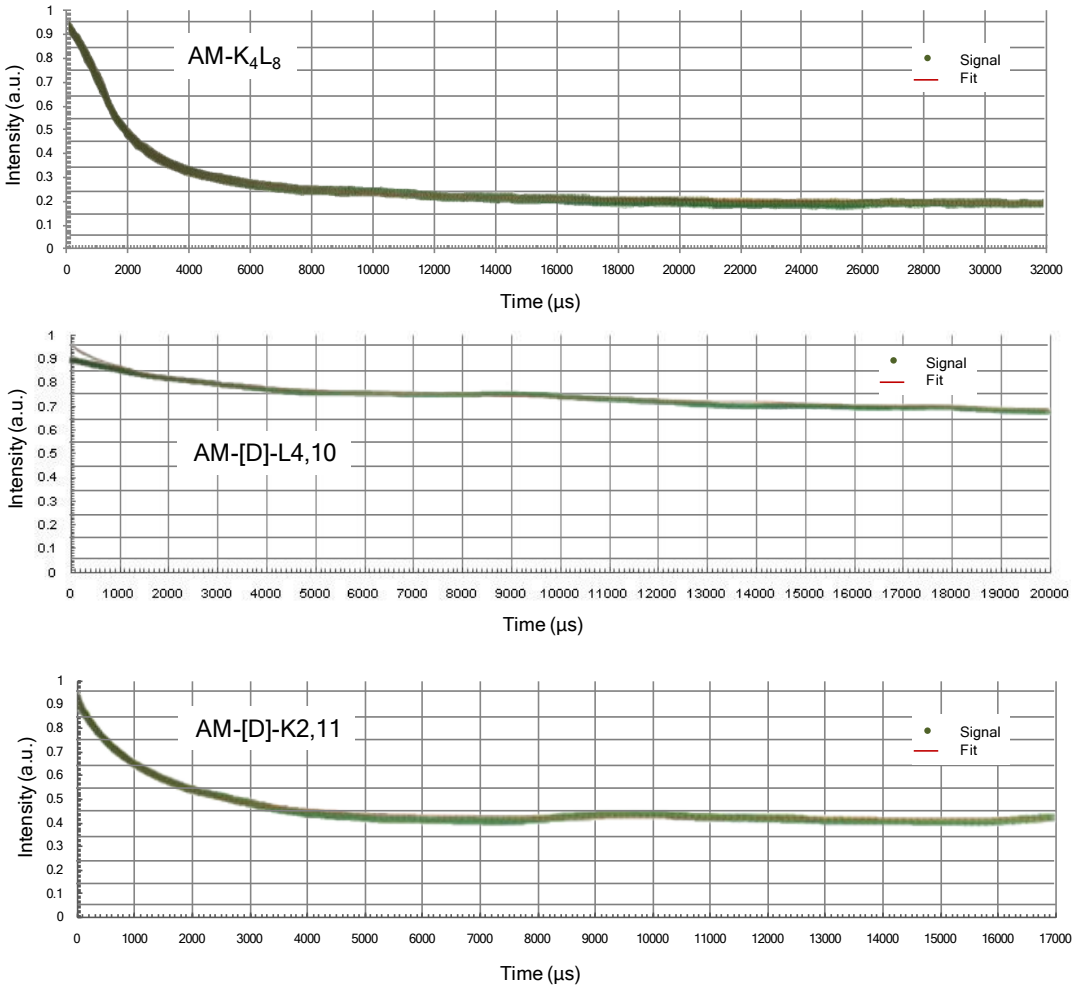

Figure S3: Representative curves of time-dependent autocorrelation function measured with DLS apparatus at scattering angel of θ=135° for amphipathic set of diastereomeric peptides. The measurements were performed in triplicates using 2.5 mg/ml of each sample. The curves demonstrate correlation between the exponential decay rate and the respective peptide structural morphology. Thus, AM-K_4L_8 peptide (rod-like fibrous morphology) exhibited the fastest exponential decay rates, whereas AM-[D]-L4,10 (crystalline morphology) is characterized by minimal decay indicating large aggregates with very low mobility. AM-[D]-K2,11 exhibited autocorrelation function decay rate to an intermediate degree.

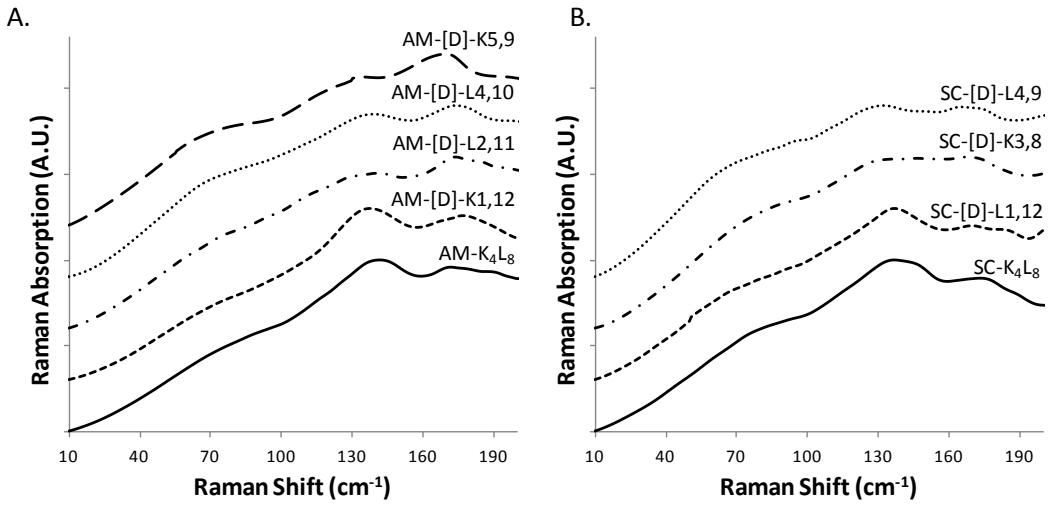

Abbreviation	Peak Center (cm^{-1}) and Qualitative Characteristic		
	~60	~135	~170
AM-[D]-$K_{5,9}$	71 (±0.5)	137 (±5.0)	175 (±4.3)
AM-[D]-$L_{4,10}$	64 (±2.6)	137 (±3.6)	171 (±4.1)
AM-[D]-$L_{2,11}$	67 (±2.4)	139 (±3.2)	178 (±2.7)
AM-[D]-$K_{1,12}$	64 (±2.1)	137 (±1.8)	169 (±4.1)
AM-K_4L_8	69 (±4.7)	139 (±2.3)	174 (±2.0)

Abbreviation	Peak Center (cm^{-1}) and Qualitative Characteristic		
	~60	~135	~170
SC-[D]-L4,9	62 (±2.3)	131 (±3.4)	172 (±1.7)
SC-[D]-K3,8	68 (±1.9)	135 (±3.7)	172 (±1.8)
SC-[D]-L1,12	69 (±2.5)	142 (±2.2)	175 (±2.2)
SC-K_4L_8	73 (±0.14)	139 (±0.4)	175 (±0.14)

Figure S4: The LF-Raman absorption modes of the amphipathic (A.) and scrambled (B.) sets of model peptides and their diastereomeric analogous. The curves are offset for better visualization of modes intensity changes between different diastereomeric peptides in the set. For each set, the below tables summarize the peak center of each individual band. The measurements were performed in triplicates using 12.5 mg/ml of each sample.

A.

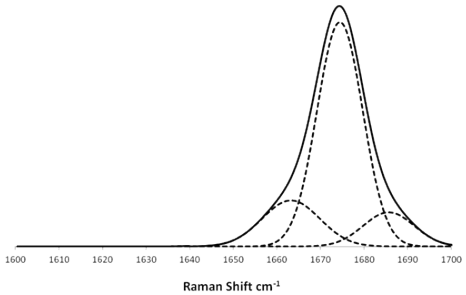

B.

Abbreviation	Unordered α-helix Center (cm^{-1})	Unordered α-helix Area (%)	β-sheet Center (cm^{-1})	β-sheet Area (%)	β-sheet Center (cm^{-1})	β-sheet Area (%)
AM-K_4L_8	1663 (± 3.1)	18 (± 8.7)	1674 (± 0.2)	70 (± 9.1)	1686 (± 0.2)	12 (± 1.3)
AM-[D]-K1,12	1662 (± 1.1)	17 (± 2.0)	1674 (± 0.1)	71 (± 2.1)	1687 (±1.3)	11 (± 1.1)
AM-[D]-L2,11	1661 (± 0.9)	19 (± 0.9)	1674 (±0.3)	69 (±0.4)	1691 (± 0.2)	12 (± 1.6)
AM-[D]-K5,9	1663 (± 1.3)	21 (± 3.0)	1675 (± 0.2)	69 (± 3.9)	1690 (± 0.2)	10 (± 1.0)
AM-[D]-L4,10	1662 (± 2.7)	19 (± 5.8)	1675 (± 0.1)	68 (± 8.0)	1690 (± 1.5)	13 (± 2.2)
SC-K_4L_8	1662 (± 0.1)	20 (± 1.0)	1674 (± 0.0)	70 (± 1.0)	1687 (±1.5)	10 (± 1.0)
SC-[D]-L1,12	1662 (± 0.0)	20 (± 5.5)	1675 (± 0.2)	68 (± 7.7)	1688 (± 1.5)	11 (± 2.2)
SC-[D]-K3,8	1663 (± 0.1)	19 (± 0.3)	1675 (± 0.1)	69 (± 2.1)	1691 (± 1.0)	12 (± 1.7)
SC-[D]-L4,9	1663 (± 0.2)	20 (± 0.4)	1674 (± 1.4)	74 (± 1.1)	1689 (± 2.3)	6.6 (± 0.7)

Figure S5: (A.) Deconvolution of the Amide I band (1600-1700 cm^{-1}) Raman spectra of the AM-K_4L_8 model peptide. The component peaks are the result of curve fitting using a Gaussian distribution. The sums of the fitted components superimpose on the experimental amide I region spectra. The solid line represents the experimental Amide I spectra after Savitzky-Golay smoothing and the dashed lines represent the fitted components. (B.) Peak center and assignment of the individual bands resolved in the amide I domain of MFM spectra obtained for the amphipathic and scrambled sets of diastereomeric model peptides. The measurements were performed in triplicates using 12.5 mg/ml of each sample